



Discrete carbon nanotubes increase lead acid battery charge acceptance and performance



Steven W. Swogger^a, Paul Everill^{a,*}, D.P. Dubey^b, Nanjan Sugumaran^{a,1}

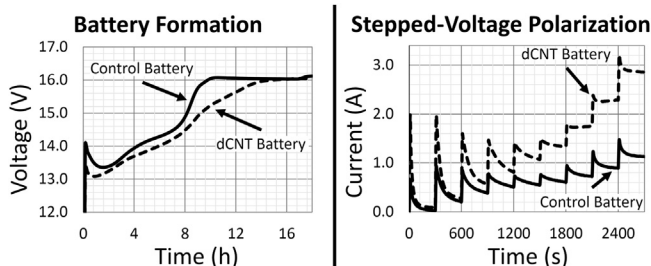
^a Molecular Rebar Design LLC – MRLead Plus, 13477 Fitzhugh Road, Austin, TX 78736, USA

^b Pacific Batteries Ltd., Lot 20/21, Wailda Industrial Estate, Lami, Fiji

HIGHLIGHTS

- Molecular Rebar[®] lead negative is a NAM additive comprising discrete carbon nanotubes (dCNT).
- dCNT can increase the charge acceptance of lead acid batteries by >200%.
- dCNT reduce energy losses of lead acid batteries >15%.
- dCNT do not change NAM paste density or rheology.
- dCNT is easily implemented in existing manufacturing processes.

GRAPHICAL ABSTRACT



ARTICLE INFO

Article history:

Received 5 February 2014

Received in revised form

12 March 2014

Accepted 14 March 2014

Available online 26 March 2014

Keywords:

Carbon nanotube

Lead acid battery

Additive

Molecular Rebar[®]

Negative active material

Charge acceptance

ABSTRACT

Performance demands placed upon lead acid batteries have outgrown the technology's ability to deliver. These demands, typically leading to Negative Active Material (NAM) failure, include: short, high-current surges; prolonged, minimal, overvoltage charging; repeated, Ah deficit charging; and frequent deep discharges. Research shows these failure mechanisms are attenuated by inclusion of carbon allotropes into the NAM. Addition of significant quantities of carbon, however, produces detrimental changes in paste rheology, leading to lowered industrial throughput. Additionally, capacity, cold-cranking performance, and other battery metrics are negatively affected at high carbon loads.

Presented here is Molecular Rebar[®] Lead Negative, a new battery additive comprising discrete carbon nanotubes (dCNT) which uniformly disperse within battery pastes during mixing. NS40ZL batteries containing dCNT show enhanced charge acceptance, reserve capacity, and cold-cranking performance, decreased risk of polarization, and no detrimental changes to paste properties, when compared to dCNT-free controls. This work focuses on the dCNT as NAM additives only, but early-stage research is underway to test their functionality as a PAM additive.

Batteries infused with Molecular Rebar[®] Lead Negative address the needs of modern lead acid battery applications, produce none of the detrimental side effects associated with carbon additives, and require no change to existing production lines.

© 2014 The Authors. Published by Elsevier B.V. This is an open access article under the CC BY license (<http://creativecommons.org/licenses/by/3.0/>).

1. Introduction

As the uses and expectations for lead acid batteries evolve, so too do their modes of failure. Traditionally, the majority of failures were related to grid corrosion and softening in the Positive Active Material (PAM) however, in contemporary applications, these have

* Corresponding author.

E-mail addresses: swswoegger@molecularrebar.com (S.W. Swogger), peverill@molecularrebar.com (P. Everill), dubey@pacificbatteries.com.fj (D.P. Dubey), nanjans@hotmail.com (N. Sugumaran).

¹ Tel.: +91 941 208 4170.

been replaced by sulfation in the Negative Active Material (NAM), acid stratification, and short-circuit producing dendrite formation [1,2]. These “contemporary applications” are defined as any in which the battery experiences: frequent, short, high-current surges during charge and discharge (ex. micro-hybrid vehicles); minimal, but consistent overvoltage charging (ex. solar/photovoltaic cells); deficit charging caused by the increased energy demands of modern electronics (ex. automotive power); or, two to three deep cycles per day (ex. motive power). Recent studies suggest that such failure mechanisms can be averted by increasing the battery’s charge acceptance, often through addition of excess carbon [3].

Carbon is added during NAM mixing as one, or a combination of, its carbon black, activated carbon, or graphite allotropes [4,5], and less commonly its graphene or nanotube allotropes. If restricted to 0.1–6.0% w.r.t. lead oxide weight, carbon is capable of doubling the battery’s charge acceptance [6,7]. Throughout that range, however, carbon steadily increases the volume of water required for paste formation leading to decreases in paste density of up to 30% [6]. Reduced paste density lowers not only plate strength, battery capacity, and cold-cranking performance, but also production throughput. Consequently, a carbon allotrope capable of boosting charge acceptance at concentrations low enough to conserve paste density and plate strength is required.

Although the concept that carbon enhances charge acceptance is universally acknowledged, controversy exists regarding which allotrope produces the best effect, and in what concentration. In early studies, carbon black is preferred [3], but later studies describe the negative impact of carbon black additions over 0.5%, w.r.t. lead oxide weight, on formation [8]. Various forms of activated carbon have since proven more beneficial than common carbon black [9,10]. Analogous studies using 2% graphite, w.r.t. lead oxide weight, find decreases in charge acceptance, but addition of 1–2% carbon black in combination with the 2% graphite successfully produces performance gains [4]. Some authors find that carbon black or graphite loaded at 3% or 6%, w.r.t. lead oxide weight, respectively, improves charge acceptance but diminishes capacity and cold-cranking performance [6]. Regardless of the allotrope or concentration, the importance of a homogenous distribution of carbon throughout the paste/plate is understood [11]. This seemingly simple stipulation is often problematic given the poor dispersibility of many forms of carbon.

The mechanism by which carbon increases charge acceptance is also disputed. Some attribute the carbon’s charge-acceptance enhancing properties to its ability to act as a fast-charging, intermediary capacitor between the source of energy and the more slowly charging lead [9,10,12,13]. Some of this capacitive effect may be due to the ability of carbon nanotubes to adsorb and reversibly store 0.1–10% hydrogen, w.r.t. carbon weight, depending on temperature, pressure, and nanotube purity [14]. Hydrogen adsorption is fast, proceeding through the Volmer–Heyrovsky mechanism on carbon, and briefly delays hydrogen gas evolution to better handle overvoltage conditions [15]. Others suggest that high surface area carbon additives increase effective NAM surface area, increasing efficiency and decreasing polarization [7,16]. Carbon could also increase charge acceptance by blocking the growth of resistive lead sulfate deposits either sterically [17–20] or electrically [3], by acting as a conductive bridge around them, to improve lead reconversion rates. Alternate functions for carbon include providing additional surface area to facilitate the deposition of lead [8,21] or, in VRLA batteries, consuming PAM-produced oxygen to limit NAM sulfation and promote water oxidation [22]. In the battery, carbon likely participates in many of these roles to various extents.

The ideal carbon additive would be uniformly distributed throughout the paste and capable of boosting charge acceptance at

concentrations low enough to avoid the decreases in paste density, cold-cranking performance, and reserve capacity experienced with current NAM additives. A recently developed carbon nanotube derivative, Molecular Rebar[®], has the potential to fulfill this ideal [23]. The associated NAM additive, Molecular Rebar[®] Lead Negative (MRLead–), is provided as a pourable, aqueous fluid comprised of surfactant-stabilized, discrete, carbon nanotubes (dCNT). The highly dispersed nature of the fluid enables additive uniformity throughout the NAM to ensure the dCNT benefits are felt plate-wide.

Here, batteries formulated with and without dCNT/Molecular Rebar[®] in the NAM are compared based on their paste mixing profile, paste density, formation profile, reserve capacity, cold-cranking performance, and, most importantly, charge acceptance.

2. Experimental

2.1. Materials

Discrete carbon nanotubes (dCNT), also known as Molecular Rebar[®], are manufactured in Austin, Texas, by Molecular Rebar Design, LLC through a proprietary process that disentangles and functionalizes stock carbon nanotubes. Functionalization includes addition of carboxylic acid groups to the surface of the tubes and an increase in the number of open ends. The process also provides additional cleaning of the carbon nanotubes such that their residual catalyst content (Fe, Al, etc.) drops ~80% from 5% by weight carbon to less than 1%, resulting in near pristine dCNT. Fig. 1 shows a comparison of stock carbon nanotubes and the dCNT known as Molecular Rebar[®] at a magnification low enough (5000×) to differentiate macrostructures. At higher resolution (>20,000×), the two samples are less distinguishable. Stock carbon nanotubes are used exclusively in paste distribution experiments and not included in any battery test.

The process by which the dCNT are prepared for use in lead acid batteries involves a surfactant coating step employing a high intensity mixer. This produces a final, fluid dispersion of dCNT, surfactant, and water at a final concentration of 3% w/v dCNT at pH 7. This fluid is named Molecular Rebar[®] Lead Negative, or MRLead–.

Lead oxide (70% PbO/30% Pb) is manufactured onsite at Pacific Batteries, Ltd from 99.97% pure lead.

Hammond Expander is purchased directly from Hammond and used as per the manufacturer’s instructions. Here, expander appropriate for SLI battery formulations is used (HEM-4640). The product includes proprietary amounts of barium sulfate (40–60%), sodium lignosulfate (25–40%), and carbon black (10–20%) [24].

All water used in the battery making process adheres to BS 4974:1975 standards.

Battery grade sulfuric acid (1.40 sp. gr.) is used during paste mixing.

2.2. Negative Active Material (NAM) paste mixing and analysis

dCNT are provided as an aqueous dispersion, MRLead–, allowing them to be uniformly distributed in NAM. During regular pasting procedures, a specific volume of water, X , is added to dry ingredients such that appropriate paste density specifications are met. To conserve paste consistency, the volume of MRLead–, Y , added to the paste is displaced from volume X to result in a remaining water allowance volume, Z , such that $X = Y + Z$. The MRLead– volume, Y , is added to the dry mixture first, followed by the remaining water allowance, Z , in order to maintain the liquid portion of the paste at volume X .

Large-scale paste mixes comprising 230 kg lead oxide and 1.4 kg Expander are combined mechanically as 27.0 L water (Control) or

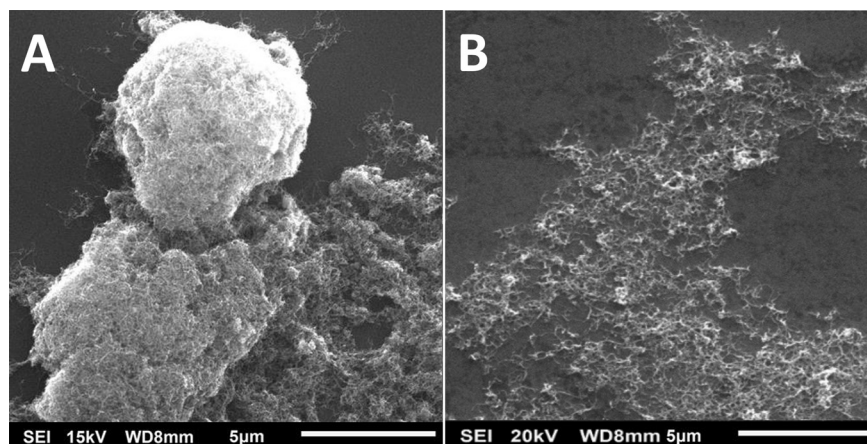


Fig. 1. SEM comparison of stock vs. discrete carbon nanotubes. A, Stock carbon nanotubes appear as bundles of entangled tubes whose aspect ratios (length/width) approach 1. B, dCNT are discrete, untangled carbon nanotubes with aspect ratios approaching 70 (typically 900×13 nm) appearing, here, as a thin mat due to an artifact of sample preparation. Images magnified $5000\times$.

14.5 L water and 12.5 L MRLead– (Experimental) are added. When a paste forms, 23.1 kg sulfuric acid is added to form the completed, pasteable dough.

Paste density is measured by volumetric cup and mass balance. Cone penetration is measured by Humboldt penetrometer.

2.3. Scanning electron microscopy

High resolution scanning electron microscopy is accomplished with a Jeol JSM-6010LV instrument.

Samples of carbon nanotubes are prepared by diluting 2–5 mg of material into 5–6 mL of isopropanol. The samples are then briefly bath sonicated before a drop of the liquid is placed on a silicon wafer and air dried. The wafer is then secured to a sample platform with colloidal graphite.

Battery plate samples are removed from their grids and briefly ground by mortar and pestle. A small piece of double-sided carbon tape is used to secure some of the resultant grains to a sample platform.

Images are typically resolved at $5\text{--}20,000\times$ magnification with a spot size of 20–30 and a beam strength of 15–20 kV.

2.4. Plate curing, battery manufacture, and formation

After paste mixing, the material is pasted onto 1.7% Sb grids where it undergoes a standard curing procedure resulting in finished plates with <1% free lead and <1% moisture.

After curing, the negative plate contains a final dCNT concentration of 0.16%, a final barium sulfate concentration of 0.24–0.37%, a final sodium lignosulfonate concentration of 0.15–0.24%, and a final carbon black concentration of 0.06–0.12%, all w.r.t. lead oxide.

NS40ZL (38B20L) batteries are defined by the Japanese Industrial Standards Committee (JISC, Standard #D 5301 2006) as 12 V, B-type, automotive batteries rated with 45 min reserve capacity, 35 Ah C_{20} rate, and 280 s cold-crank performance. NS40ZL dimensions are: length, 197 mm; width, 129 mm; and height, 230 mm. NS40ZL batteries with and without dCNT in the negative plate are produced at Pacific Batteries Ltd. (Lami, Fiji) and shipped to an independent battery research laboratory, JBI Corporation (Ohio, USA), for formation and testing. Each NS40ZL cell contains 4 positive and 5 negative plates. The positive plates, also manufactured at Pacific Batteries Ltd., contain no expander and no dCNT.

Batteries are flooded and formed at JBI Corporation using 7 A constant current over 18 h. Voltage evolution is monitored every

10 min. Formation data is the average of 5 concurrently tested batteries.

2.5. Battery testing regimen

All battery data is an average of five concurrently tested batteries. Prior to testing, all batteries are fully charged using a constant voltage of 14.8 V and a limiting current of 8 A for 20 h. Batteries are allowed to cool for 4 h prior to use.

Freshly formed batteries are subjected to alternating cycles of reserve capacity and cold-cranking measurement. A total of three cycles (3 RC and 3 CCA) are presented.

2.5.1. Reserve capacity test

Batteries are discharged at 25 A constant current until voltage decreases to 10.5 V. Time is measured. Prior to cold-cranking tests, batteries are recharged using 14.8 V constant voltage with a limiting current of 8 A for 20 h followed by a 4 h cooling period.

2.5.2. Cold-cranking performance tests

Batteries are discharged at -18°C with a 270 A constant current. The voltage after 30 s is measured. Additionally, the length of time required to discharge the battery to 6.0 V is also measured. After this test, batteries are recharged using 14.8 V constant voltage with a limiting current of 8 A for 12 h.

2.6. Polarization tests, constant voltage and constant current

Polarization tests are conducted after the Battery Testing Regimen described in Section 2.5. Prior to tests, all batteries are fully charged using a constant voltage of 14.8 V and a limiting current of 8 A for 20 h. Batteries are cooled for 4 h prior to use. All data represents an average of five concurrently tested batteries.

In constant current studies, a set current is sent through fully charged batteries for 5 min during which time voltage is measured. After the first 5 min, the current is raised, and voltage is measured again for a second 5 min period. This protocol repeats for a total of 10 measurements. Here, the current profile begins at 0.2 A and rises in 0.2 A increments until a final current of 2.0 A is reached.

A Tafel Plot is extrapolated from the above data set using the calculated overvoltage at each 5 min period versus the logarithm of the current over that particular period.

In constant voltage studies, a set voltage of 13.0 V is placed over fully charged batteries with a limiting current of 7 A applied.

Current is monitored for 5 min and then the voltage is increased by 0.3 V. Current is monitored again for 5 min, and this trend continues with 0.3 V boosts until a final voltage of 15.4 V is reached.

Steady-state constant voltage tests, are extrapolated from the above data set using the final current measurement of each 5 min period versus the voltage of that particular period.

2.7. Cold charge acceptance

Fully charged batteries are discharged at a constant current of 3.5 A for 5 h or until they reach 50% State of Charge (SoC). Batteries are then cooled to 0 °C over 18 h. Charging proceeds at a constant voltage of 14.4 V with current input being measured for 10 min. Curve shape, current end point, and Ah forced into the battery are examined.

3. Results and discussion

3.1. dCNT are better distributed in the plate than stock CNT

In order to highlight the advantages of dCNT additives (ex. MRLead-) over stock carbon nanotube-based additives, pastes were mixed using identical formulations of each material and compared. Each carbon nanotube variety is included at a final concentration of 0.16% w.r.t. lead in their respective pastes. After drying, the complete pastes are ground by mortar and pestle to be visualized by SEM.

Images taken of the paste comprising stock carbon nanotubes show large agglomerations of tubes with some single nanotubes protruding from them (Fig. 2Aⁱ⁻ⁱⁱ). In all micrographs gathered (not all shown), most nanotubes are within, or close to, agglomerations; few are found individualized. Such agglomerations concentrate the nanotubes in small areas and limit the additive's uniformity within the paste/plate. Although the larger balls depicted in Fig. 1A have clearly decreased in size, an effect of shearing applied by lead crystals and mixing equipment, they are far from the loosely-

arranged, discrete tubes shown in Fig. 1B. For full effect, the carbon nanotubes need to be well dispersed throughout the paste, bridging lead crystals or forming points of nucleation. Isolated pockets of nanotubes could result in plate "hot spots" possibly leading to increased stratification or uneven plate utilization.

Fig. 2Bⁱ⁻ⁱⁱ show dried, ground paste containing dCNT. Here, the nanotubes appear mostly as singular entities. Some are seen wrapped around lead crystals, others lie along the surface, but in no micrograph (not all shown) are they seen as larger clusters. The increased uniformity achievable with dCNT is explained with three observations: 1) the dCNT present in MRLead- are individual, surfactant-stabilized entities unlikely to migrate together, 2) although some dCNT surface carboxylic acid groups may be masked by surfactant, tubes with these functionalities have shown increased ability to bind lead, likely favoring dCNT-lead over dCNT-dCNT interactions during mixing which lowers nanotube aggregation [25,26], and 3) MRLead- is provided as a liquid which is more easily incorporable into mixtures than a solid.

Use of dCNT, instead of stock or unformulated carbon nanotubes, results in an improved distribution of nanotubes throughout the battery paste which ensures that any positive effects are felt uniformly and plate-wide, possibly protecting against polarization or incomplete plate utilization.

3.2. Effect of dCNT on paste rheology and consistency

Addition of excess carbon additives usually demands the addition of excess water to complete paste formation [4]. Negative effects of this procedure include decreased paste density, decreased plate strength, and alterations to the industrial process to accommodate these changes. Pastes including dCNT at a final concentration of 0.16% w.r.t. lead oxide were produced and compared with CNT-free control pastes to screen for these effects.

An industrial-scale pasting mixer's motor current profile is revealing of the paste's physical characteristics. Both mixtures require the same amount of liquid for a paste to form, be it water

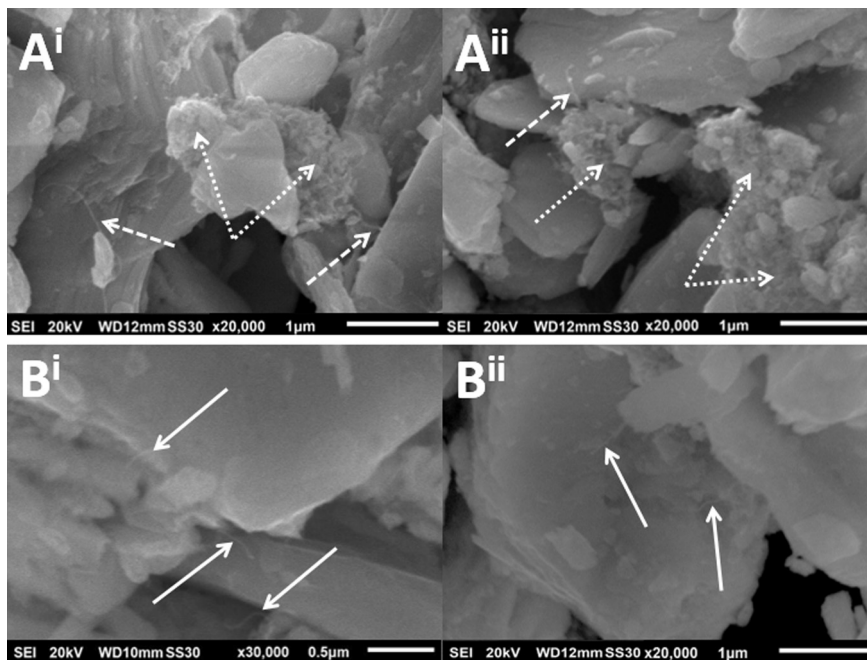


Fig. 2. dCNT incorporate uniformly into pastes. Aⁱ⁻ⁱⁱ, Micrographs of paste mixed with stock carbon nanotubes at 0.16% w.r.t. lead show entangled balls of nanotubes (dotted arrows) and a few single nanotubes protruding from them (dashed lines). Bⁱ⁻ⁱⁱ, Micrographs of paste mixed with dCNT at 0.16% w.r.t. lead show discrete nanotubes (solid arrows) along the surface of the lead particles or trapped between them. No tangled balls are observed in micrographs retrieved from the dCNT paste sample. Images magnified 20–30,000×.

and acid, or a combination of water, MRLead–, and acid. Fig. 3 compares the current profile of pastes mixed with and without dCNT. The traces are similar in shape showing that both mixtures undergo similar changes in consistency during the process. On average, a ~2% difference is observed between the two indicating that the additive does not substantially change paste rheology. A 2% difference is within the region of mechanical fluctuation.

Other comparative parameters include paste density and paste penetration. After mixing, no difference is observed in paste density; the value with or without dCNT is $4.20 \pm 0.01 \text{ g cc}^{-1}$. Similarly, there is no change in paste penetration. The value for control batteries is indistinguishable from batteries containing dCNT, set at 19 units.

With no significant changes to rheology, density, or penetration, incorporation of dCNT will require no changes to existing paste mixing, pasting, or manufacturing processes.

3.3. Effect of dCNT on cured negative paste structure

With no observable effect on the macroscopic paste level, the microscopic crystalline level is next explored.

Scanning Electron Microscopy (SEM) images of ground, cured, negative paste show that dCNT change the microstructure of the material (Fig. 4). Further inspection of the plates reveals that dCNT produce a more ordered geography than control, CNT-free plates that may increase plate porosity. These pores and crevices are noticeable in Fig. 4B as darker regions on the micrograph and are sharply contrasted from the landscape shown in Fig. 4A which appears fluffier, with more loosely defined three dimensional structures. Future images of formed, cycled, negative plates or surface area analyses may intensify these differences and confirm the link between dCNT addition and increases plate porosity.

On a procedural aside, plates containing dCNT are noticeably harder to break by hand than CNT-free control plates, possibly hinting at a role for dCNT in increasing plate strength. This parameter is not rigorously tested here.

SEM micrographs suggest that addition of dCNT plays a role in plate porosity, possibly leading to changes in material utilization when electrolyte gains access to previously unreachable areas of the plate. Importantly, this change in microstructure and,

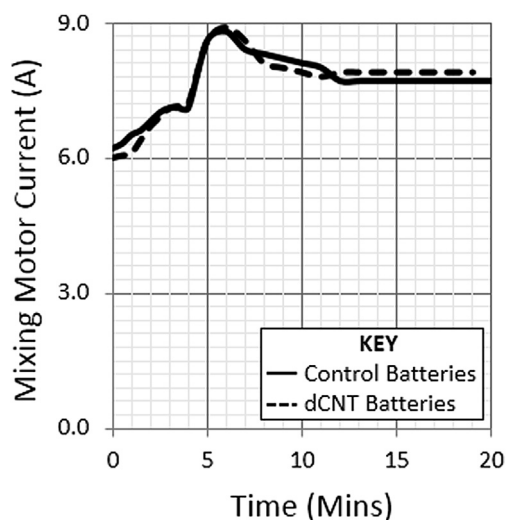


Fig. 3. MRLead– does not affect mixing motor current profiles. The current required to mechanically mix CNT-free lead pastes or lead pastes containing dCNT differ by an average of ~2%, within the region of mechanical fluctuation, along the length of the trace.

potentially, porosity is accomplished without detrimental changes to paste/plate density which differentiates dCNT from previous carbon additives. Increases in utilization can be followed by increases in capacity; a parameter evaluated here later.

3.4. Effect of dCNT on cured, unformed, negative plate formation

Fig. 5 compares the constant-current charging profile of control, CNT-free batteries to batteries containing dCNT. During the formation, batteries containing dCNT require lower voltages indicative of a less resistive, more easily chargeable matrix. The gap in charging voltages varies by as much as 860 mV.

The decrease in charging voltage for batteries containing dCNT delays the onset of gas evolution. In the positive plate, oxygen is generated at a voltage of 14.4 V and has a destructive effect on the PAM. Batteries containing dCNT reach that potential ~2 h (~11% of the total charging time) later than controls. With the positive plate in a healthier state for longer, the battery can charge more efficiently. A similar and related observation is apparent when considering the negative plate: hydrogen generation usually occurring at 16 V is delayed ~5 h (~28% of the total charging time) by the inclusion of dCNT. This delay increases the health of the negative plate, also enabling the battery to charge more efficiently. Delayed hydrogen evolution voltages could hint at increased hydrogen adsorption and storage on the surface of the dCNT. Given that the two plates function as one system, improvements in gas evolution in the positive plate are likely correlated to improvements at the negative plate. In order to quantify the levels of hydrogen and oxygen generation from batteries with and without dCNT to validate this theory, gassing studies are currently underway.

dCNT decrease the voltages required during formation and delays the onset of overvoltage-related side reactions such as gassing to increase the efficiency of the process. The change in plate microstructure for dCNT-containing batteries (Section 3.3) is likely one of the contributors to formation improvement but other metrics, such as polarization or charge acceptance, could be playing a role.

3.5. Effect of dCNT on battery performance

With positive changes evident in plate structure and formation, additional battery metrics are tested.

Fig. 6A compares reserve capacity measurements from batteries with and without dCNT over three cycles. A marginal improvement of ~1–2% is observed in the reserve capacity of batteries containing dCNT when compared to CNT-free controls. Although a minor increase, this result is important because, as mentioned previously, carbon additives from the literature tend to negatively impact this parameter. dCNT have a non-negative effect on reserve capacity.

Cold-cranking performance is also frequently hindered by excess carbon additives. Here, dCNTs have an unexpectedly positive effect on two cold-cranking metrics: duration and voltage. Fig. 6B shows that inclusion of dCNT into battery plates produces a ~6–10% increase in the length of time taken to decrease the battery voltage to 6 V at 270 A in a -18°C environment across the three cycles.

dCNT batteries also produce a marginal (~2%) increase in the voltage produced after a 30 s discharge at 270 A in a -18°C environment as shown in Fig. 6C. These data indicate that batteries containing dCNT perform comparably, or slightly better than, CNT-free control batteries in cold conditions. This is, again, surprising given the negative effects of excess carbon usually encountered in cold-cranking tests.

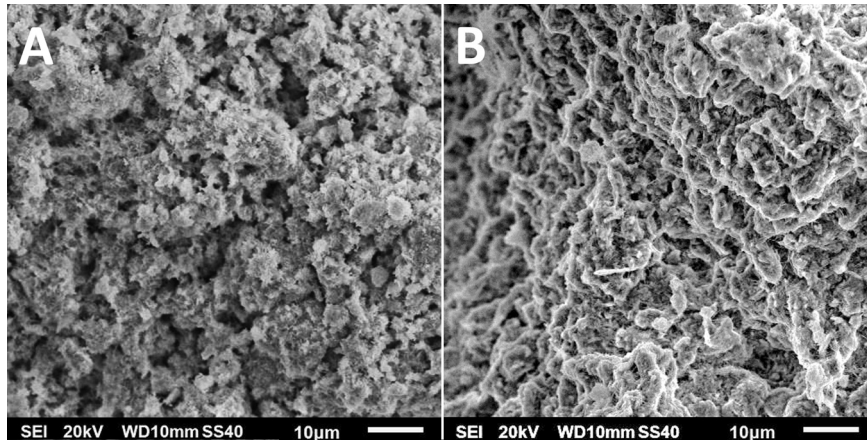


Fig. 4. dCNT change NAM plate microstructure. A, Cured, ground, NAM plates in the absence of dCNT show fluffier, poorly defined structures. B, Cured, ground, NAM plates in the presence of dCNT show tighter, well-defined structures with deeper/darker pore structures. Images magnified 1000 \times .

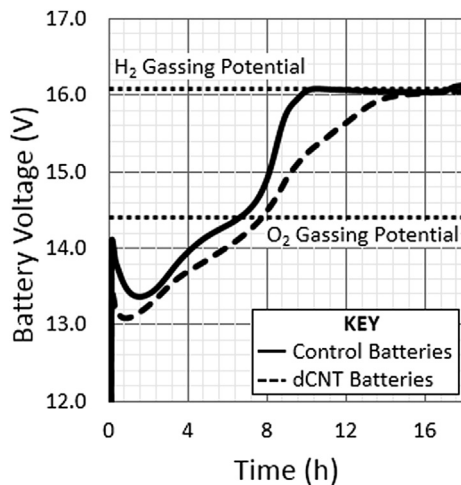


Fig. 5. Effect of dCNT on battery formation. During an 18 h, 7 A constant current formation, both CNT-free control and batteries containing dCNT reach gas evolution. The gap in charging voltages varies by as much as 860 mV and indicates more efficient charge acceptance that requires less voltage to push the same current in dCNT batteries. Inclusion of dCNT delays the onset of O₂ evolution by 2 h (11%) and H₂ evolution by 6 h (28%) to limit PAM degradation and gassing, respectively.

Over the three reserve-capacity/cold-cranking cycles, charge input and output was recorded in terms of Ah. These values are summed and presented in Fig. 6D. Batteries containing dCNT allow for ~15% more charge to be absorbed and ~3% more charge to be used during tests than control batteries. This improvement in charge passage has obvious ramifications for charging speed, charge utilization, and most modern applications.

Performance tests designed to compare CNT-free, control batteries with batteries containing dCNT indicate that the additive has a non-detrimental effect on reserve capacity and a positive effect on cold-cranking ability. dCNT unexpectedly improves cold-cranking metrics when other carbon-based additives in the literature led to their deterioration. Furthermore, batteries incorporating dCNT absorb and distribute more charge than control batteries under the same situations.

3.6. Effect of dCNT on battery polarization

To address the mechanism of dCNT battery performance enhancement, we undertook various polarization studies.

A decrease in the voltage required to reach each current is observed for batteries containing dCNT, compared to CNT-free controls, during the constant-current, voltage–time transient polarization test of Fig. 7A. The observation is shadowed by the Tafel Plot in Fig. 7B. The altered slope observed in the Tafel Plot of batteries containing dCNT indicates that different chemical processes are at work during overvoltage conditions. Among other possibilities, one such chemical process change could include a switch from the Volmer–Tafel mechanism to the Volmer–Heyrovsky mechanism of hydrogen evolution [15]. In the former, the rate determining step involves the formation of an adsorbed hydrogen (H_{ad}) which is followed by quick recombining of two H_{ad} to form H₂ on the lead surface, but in the latter, the formation of H_{ad} is fast but is followed by a slow recombining of an H⁺ with an H_{ad} to form H₂ on the dCNT surface. In batteries containing dCNT, the overvoltage generated is over lower magnitude than in control batteries meaning that overvoltage-dependent side reactions are proceeding through a different path.

In the constant-voltage, current–time transient polarization test of Fig. 7C, more current is passed at each voltage for batteries containing dCNT, compared to controls. The initial surge in current for batteries containing dCNT indicates an especially high charge acceptance over short durations, with obvious implications for applications involving High-Rate, Partial State of Charge (HRPSoC) or deficit-charging. This observation could further substantiate the intermediary/super capacitor effect of carbon claimed by some [9,10,12,13]. The constant-voltage, steady-state polarization test of Fig. 7D reiterates the result of Fig. 7C: the voltage required to achieve the set currents is decreased which increases battery efficiency and could allow for new battery designs or charging specifications.

The constant current and constant voltage polarization studies corroborate each other and show that batteries containing dCNT are capable of dealing more effectively with high current and overvoltage. By limiting overvoltage situations, the batteries better resist polarization-inducing side reactions. For example, while control batteries produce 1 A at 15 V (2.4 V overvoltage), batteries containing dCNT can produce the same current at 14.5 V (1.9 V overvoltage), a ~21% reduction in overvoltage (Fig. 7B). Batteries operating in HRPSoC, for example, should gain increases in lifetime by virtue of more efficient charging at lower voltages and decreases in overvoltage-based side reactions like gassing, stratification, or polarization.

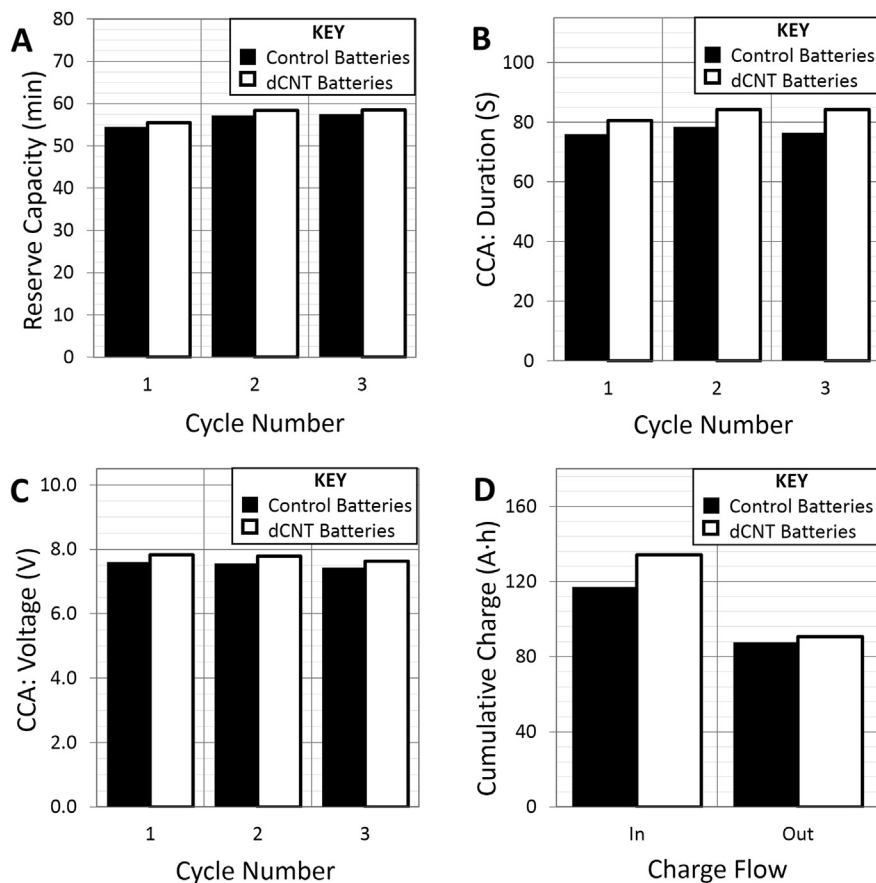


Fig. 6. Effect of dCNT on NS40ZL battery performance and charge acceptance. A, Reserve capacity tests (25 A discharge until voltage < 10.5 V) show slightly increased capacity in batteries containing dCNT over CNT-free controls. B, Cold-cranking, durational tests (270 A discharge until voltage < 6 V at -18°C) show that batteries containing dCNT persist ~ 7 – 10% longer than CNT-free controls. C, Cold-cranking, voltage tests (270 A discharge at -18°C , voltage read at 30 s) show marginal increases in voltage from batteries containing dCNT. D, The cumulative charge factor, the total charge passing in and out of the batteries during three cycles of recharging, reserve capacity, and cold-cranking studies, shows batteries containing dCNT absorb $\sim 15\%$ and pass $\sim 3\%$ more charge than CNT-free controls.

3.7. Effect of dCNT on cold charge acceptance

The unexpected improvement in cold-cranking performance (Section 3.5/ Fig. 6B–C) initiated a further experiment to test the performance of batteries containing dCNT in colder environments, specifically with regard to their charge acceptance.

Fig. 8 shows the current input to a battery charging from a 50% SoC at a constant voltage of 14.4 V in a 0°C environment. Although the shape of the dCNT battery current trace is similar to that of the control battery, a marked increase in current input is observed for the dCNT battery over the entire 10 min charge. At the 10 min (600 s) mark, the control battery is absorbing a current of 6.68 A while the battery containing dCNT is absorbing 7.55 A; a 13% increase in current input. The area under the curve (AUC) is equal to the total charge accepted by the battery in units of A s and are easily converted to Ah. As indicated on the graph, control batteries absorb 1.33 Ah over the 10 min charge while batteries containing dCNT absorb 1.41 Ah; a 6.01% increase in charge accepted.

Here, further improvements in cold temperature battery performance are identified: batteries built with dCNT channel larger currents to accept more charge than control batteries at 0°C . These data add to earlier observations that batteries containing dCNT produce higher voltage and endure longer at -18°C than control batteries. A boost in cold temperature performance metrics is an unexpected benefit of dCNT, one that differentiates them from other forms of carbon additive, and increases their utility.

4. Conclusions

Presented here is a brief and ongoing study of Molecular Rebar[®] Lead Negative, a new NAM additive comprised of discrete carbon nanotubes (dCNT).

dCNT are shown to be uniformly dispersed into lead acid battery pastes in a manner which does not affect paste rheology, density, or consistency. Cured dCNT-laced plates appear more porous in SEM micrographs, indicative of their potential for increased utilization and capacity. When batteries containing dCNT are formed, they require less voltage than CNT-free control batteries in a process which could decrease formation time, reduce formation costs, and increase plant capacity. Lowered formation voltage also decreases the length of time spent in overvoltage conditions and, in turn, decreases plate deterioration, leading to a more efficient process. Contrary to other carbon additives mentioned in the literature, dCNT do not negatively impact reserve capacity or cold-cranking performance, instead improving these battery metrics ~ 1 – 10% over CNT-free controls. The positive results gathered from cold condition tests are surprising given that many carbon additives reduce the performance of batteries in such environments. Here, dCNT batteries produce higher voltages over longer durations at -18°C and accept more charge at 0°C than control batteries. Polarization studies show that dCNT incorporation allows batteries to channel up to $\sim 200\%$ more current at the same voltage, or produce $\sim 21\%$ less overvoltage at the same current, than control

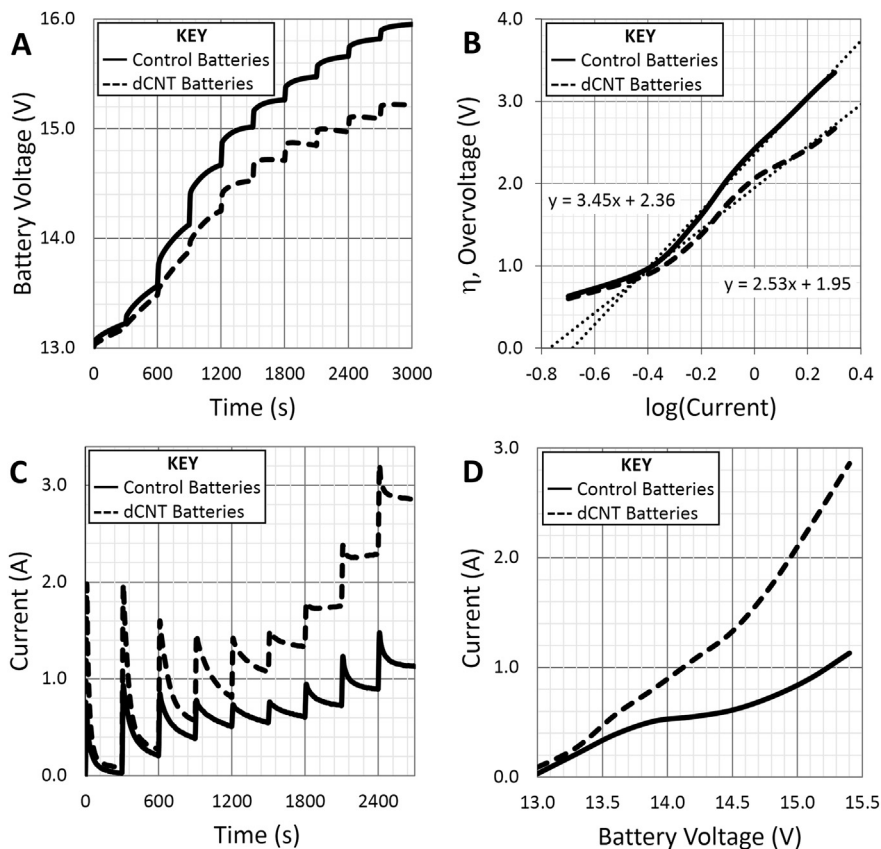


Fig. 7. Effect of dCNT on battery polarization. A, In constant-current studies (voltage measured, current increased from 0.2 to 2 A in 0.2 A, 5 min increments), batteries containing dCNT exhibit less overvoltage than CNT-free controls, indicative of more efficient charge acceptance. B, A Tafel Plot extrapolated from A reiterates that batteries containing dCNT absorb the same current as CNT-free control batteries but at lower voltages. Tafel Plot slope variances indicate different overvoltage processes occurring in batteries containing dCNT, possibly involving hydrogen storage. C, In constant-voltage studies (current measured, voltage increased from 13 to 15.4 V in 0.3 V, 5 min increments), batteries containing dCNT produce almost 200% more current than CNT-free controls. The initial, strong current spike suggests a supercapacitive role for dCNT. D, Constant-voltage, steady-state studies confirm batteries containing dCNT pass almost 200% more current than CNT-free controls.

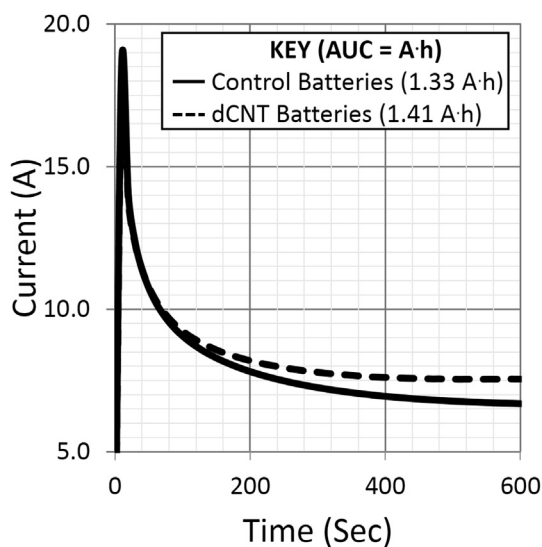


Fig. 8. Effect of dCNT on cold charge acceptance. batteries containing dCNT charging from a 50% SoC at a constant voltage of 14.4 V in 0 °C temperatures absorb more current than control batteries. After 10 min of charge, control batteries are adsorbing 6.68 A of current whereas batteries containing dCNT adsorb 7.55 A (13% increase). Area under the curve calculations show that dCNT batteries accept 6.01% more charge than control batteries over the same period (1.33 Ah vs. 1.41 Ah).

batteries. Higher charge acceptance lowers the severity of the side-effects associated with overvoltage and will likely lead to increases in battery cycle life (Data in Process). Considering the data presented here, dCNT appear to have all of the benefits of carbon additives at a low enough active concentration such as to present none of their weaknesses.

In batteries containing dCNT, a delay in reaching expected gassing voltages (oxygen = 14.4 V, hydrogen = 16 V) and a lowered Tafel slope are observed. These changes indicate a shift in the chemistry of the battery, possibly to one favoring Volmer-Heyrovsky hydrogen gas evolution on the surface of the dCNT over the more commonly observed Volmer–Tafel hydrogen gas evolution on the surface of the lead. This theory, although not directly tested here, could explain the increase in charge acceptance using a mechanism involving the rapid pseudo capacitance of dCNT–hydrogen conjugates. Gassing and voltammetry tests are currently underway to examine this theory.

The greater than 200% increase in charge acceptance exhibited in batteries containing dCNT reduces the time and energy required to reach maximum charge by making the process more efficient. Modern applications including HRPSoc systems, solar energy conversion, deficit charging in automotive electronics, and others will benefit from the observed ~15% increase in cumulative charging factor. Faster charging with lower risk of polarization, stratification, or gassing is expected to increase the lifetime of the battery in these applications (Data in Process). Decreased polarization and higher charge acceptance has been directly linked to decreases in NAM sulfation and acid stratification; two

mechanisms at the heart of modern lead acid battery failure [3]. Both polarization and charge acceptance improvements are observed here with the use of dCNT, suggesting its role in attenuating one, or both, of these failure mechanisms. Furthermore, batteries infused with dCNT will exhibit at least a 10% increase in power and faster charging, over control batteries, in colder temperatures. In these ways, addition of the discrete carbon nanotubes to existing lead acid battery technology could allow for presently unmet performance demands to be satisfied. Direct testing of dCNT in HRPSOC and solar models is currently underway.

Future research includes the testing of new formulations of Molecular Rebar[®] Lead Negative, incorporation of higher dCNT content into the NAM, and the inclusion of dCNT in the PAM electrode alone, and both the NAM and PAM electrodes together.

Acknowledgments

The authors sincerely thank Kurt W. Swogger and Dr. Clive P. Bosnyak for their patronage as well as the many helpful discussions which made this research possible. The authors would also like to thank Michael Gauthier for his assistance in preparing the Molecular Rebar[®] Lead Negative for use in this study. Finally, the authors thank Mr. Vinal V. Deo and Mr. Tula Ram who provided assistance for testing the batteries at Pacific Batteries, Ltd.

References

- [1] K. Nakamura, M. Shiomi, K. Takahashi, M. Tsubota, *J. Power Sources* 59 (1996) 153–157.
- [2] J. Dambrowski, Deutronic Elektronik GmbH, Adlkofen, 2009, pp. 1–16, available at: http://www.deutronic.com/fileadmin/images/PDF/Ladegeraete/deutronic-lader_eng.pdf (accessed 03.11.14).
- [3] M. Shiomi, T. Funato, K. Nakamura, K. Takahashi, M. Tsubota, *J. Power Sources* 64 (1997) 147–152.
- [4] D.P. Boden, D.V. Loosemore, M.A. Spence, T.D. Wojcinski, *J. Power Sources* 195 (2010) 4470–4493.
- [5] D.G. Enos, S.R. Ferreira, R. Shane, Sandia National Laboratories, Albuquerque, 2011, available at: <http://prod.sandia.gov/techlib/access-control.cgi/2011/118263.pdf> (accessed 03.11.14).
- [6] W.J. Murray, S.F. Malo, in: 2011 NDIA Ground Vehicle Systems Engineering and Technology Symposium, Dearborn, Michigan, 2011.
- [7] J. Valenciano, A. Sanchez, F. Trinidad, A.F. Hollenkamp, *J. Power Sources* 158 (2006) 851–863.
- [8] D. Pavlov, T. Rogachev, P. Nikolov, G. Petkova, *J. Power Sources* 191 (2009) 58–75.
- [9] J. Xiang, P. Ding, H. Zhang, X. Wu, J. Chen, Y. Yang, *J. Power Sources* 241 (2013) 150–158.
- [10] D. Pavlov, P. Nikolov, *J. Power Sources* 242 (2013) 380–399.
- [11] E. Ebner, D. Burrow, A. Berger, M. Wark, P. Atanassova, J. Valenciano, *J. Power Sources* 239 (2013) 483–489.
- [12] M. Fernandez, J. Valenciano, F. Trinidad, N. Munoz, *J. Power Sources* 195 (2010) 4458–4469.
- [13] P.T. Moseley, *J. Power Sources* 191 (2009) 134–138.
- [14] E. Frackowiak, F. Béguin, *Carbon* 40 (2002) 1775–1787.
- [15] P.P. Prosini, A. Pozio, S. Botti, R. Ciardi, *J. Power Sources* 118 (2003) 265–269.
- [16] R.H. Newnham, W.G.A. Balasing, A.F. Hollenkamp, O.V. Lim, C.G. Phyland, D.A.J. Rand, J.M. Rosalie, D.G. Vella, in: A.L.A.B. Consortium (Ed.), Project C/N 1.1, CSIRO Energy Technology, Clayton South, 2002.
- [17] M. Calabek, K. Micka, P. Krivak, P. Baca, *J. Power Sources* 158 (2006) 864–867.
- [18] K. Micka, M. Calabek, P. Baca, P. Krivak, R. Labus, R. Bilko, *J. Power Sources* 191 (2009) 154–158.
- [19] P. Baca, K. Micka, P. Krivak, K. Tonar, P. Toser, *J. Power Sources* 196 (2011) 3988–3992.
- [20] P. Krivak, K. Micka, P. Baca, K. Tonar, P. Toser, *J. Power Sources* 209 (2012) 15–19.
- [21] D. Pavlov, P. Nikolov, T. Rogachev, *J. Power Sources* 195 (2010) 4444–4457.
- [22] K.R. Bullock, *J. Power Sources* 195 (2010) 4513–4519.
- [23] K.W. Swogger, C.P. Bosnyak, in: 70th Annual Technical Conference of the Society of Plastics Engineers, Curran Associates, Inc, Orlando, Florida, 2012, pp. 448–451.
- [24] D.P. Boden, *J. Power Sources* 73 (1998) 89–92.
- [25] M.A. Atieh, O.Y. Bakather, B. Al-Tawbini, A.A. Bukhari, F.A. Abuilawi, M.B. Fettouhi, *Bioinorg. Chem. Appl.* (2010) 603978.
- [26] H. Tahermansouri, M. Beheshti, *Bull. Kor. Chem. Soc.* 34 (2013) 3391.